Beyond blobs in percolation cluster structure: The distribution of 3-blocks at the percolation threshold

Gerald Paul* and H. Eugene Stanley
Center for Polymer Studies and Department of Physics, Boston University, Boston, Massachusetts 02215
(Received 8 February 2002; published 20 May 2002)

The incipient infinite cluster appearing at the bond percolation threshold can be decomposed into singly connected ''links'' and multiply connected ''blobs.'' Here we decompose blobs into objects known in graph theory as 3-blocks. A 3-block is a graph that cannot be separated into disconnected subgraphs by cutting the graph at two or fewer vertices. Clusters, blobs, and 3-blocks are special cases of k-blocks with $k=1$, 2, and 3, respectively. We study bond percolation clusters at the percolation threshold on two-dimensional (2D) square lattices and three-dimensional cubic lattices and, using Monte Carlo simulations, determine the distribution of the sizes of the 3-blocks into which the blobs are decomposed. We find that the 3-blocks have fractal dimension $d_3=1.2\pm0.1$ in 2D and 1.15 ± 0.1 in 3D. These fractal dimensions are significantly smaller than the fractal dimensions of the blobs, making possible more efficient calculation of percolation properties. Additionally, the closeness of the estimated values for d_3 in 2D and 3D is consistent with the possibility that d_3 is dimension independent. Generalizing the concept of the backbone, we introduce the concept of a ''k-bone,'' which is the set of all points in a percolation system connected to k disjoint terminal points (or sets of disjoint terminal points) by k disjoint paths. We argue that the fractal dimension of a k-bone is equal to the fractal dimension of k-blocks, allowing us to discuss the relation between the fractal dimension of k-blocks and recent work on path crossing probabilities.

DOI: 10.1103/PhysRevE.65.056126 PACS number(s): 64.60.Fr, 05.45.Df, 64.60.Ak

I. INTRODUCTION

Percolation is the classic model for disordered systems [1–3]. For concreteness we will study bond percolation systems in which bonds on a lattice are randomly occupied with probability p. Clusters are defined as groups of sites and bonds which are connected by occupied bonds. Clusters can be decomposed into objects known as blobs. Blobs are sets of sites and bonds which cannot be decomposed into disconnected sets by cutting only one bond. Equivalently blobs are sometimes described as being multiply connected—there are at least two disjoint paths between each point in a blob and every other point in the blob. The decomposition of the entire percolation cluster into blobs has been extensively studied [4], as has been the distribution of sizes of blobs in the backbone [5]. For both cluster and backbone blobs, the fractal dimension of the blobs is the fractal dimension of the backbone.

Here we address the questions of (i) whether there are more fundamental objects into which blobs can be decomposed, and (ii) whether these objects then be further decomposed. To answer these questions, we employ the language of graph theory, in which sites are the vertices and bonds are the edges of a graph [6].

One can define k-connected graphs (or k-blocks) as graphs that cannot be separated into disconnected subgraphs by cutting the graph at fewer than k vertices [6,7]. Thus, clusters are 1-blocks and blobs are 2-blocks. The natural next level of decomposition of percolation systems is to decompose blobs (2-blocks) into 3-blocks. By the definition above, 3-blocks are graphs that cannot be decomposed by cutting the graphs at fewer than three vertices. From a physicist's point of view, one can understand what 3-blocks are by considering a blob as a resistor network with each bond being a resistor. Assume one is trying to determine the resistance between two vertices of the network. One can simplify the network by using Kirchoff's Laws to replace groups of sequential bonds and groups of parallel bonds by single virtual bonds having resistance equivalent to the bonds replaced. After this has been done as completely as possible, what are left are 3-blocks. We define the mass of a 3-block as the number of virtual bonds plus the number of nonreplaced original bonds remaining in the 3-block. Figures 1 and 2 provide examples of the decomposition of a blob into 3-blocks. It has been shown [6] that the decomposition of 2-blocks into 3-blocks is unique.

Determining the scaling of the distribution of the 3-blocks into which the 2-blocks can be decomposed is the subject of this paper. In graph theory, the sites are typically not constrained to a lattice structure, and one is only concerned with the topology of the graphs; we will, however, work on square and cubic lattices.

II. NOTATION

Since we deal with a number of different types of fractal objects, we employ the following notation.

(i) The fractal dimension of an object of type X will be denoted as d_X.

(ii) The number distribution of objects of type X in space of type Y of size L will be denoted as $n(N_X, L_Y)$.

(iii) The exponent of the power-law regime of a distribution of objects of type X in space of type Y will be denoted as $\tau_{X,Y}$.

*Electronic address: gerryp@bu.edu

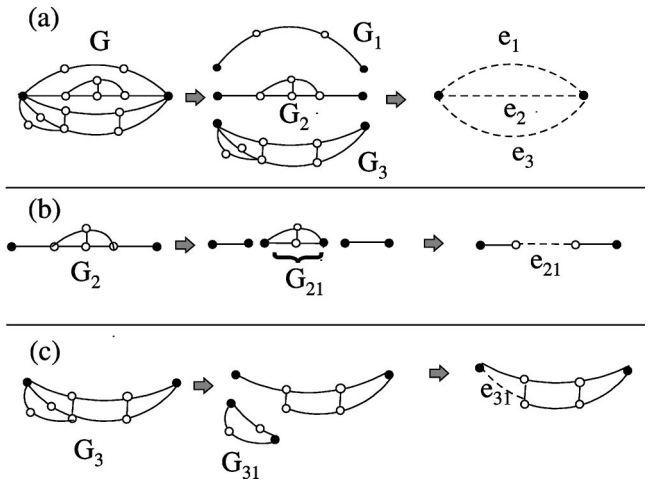

FIG. 1. (a) Decomposition of 2-block G into subgraphs G_1, G_2, and G_3. The rightmost graph represents G with the subgraphs replaced by equivalent "virtual edges." (b) Subgraph G_2 of G is decomposed by identifying subgraph G_{21}. The rightmost graph represents G_2 with the subgraph G_{21} replaced by its equivalent edge. (c) Subgraph G_3 of G is decomposed by identifying subgraph G_{31}. The rightmost graph represents G_3 with the subgraph G_{31} replaced by its equivalent edge. In (a), (b), and (c) virtual edges are denoted by dashed lines. Note that while not shown in this figure, subgraph G_{31} could be further decomposed. The 3-blocks contained in the graph G are G_{21}, having five edges, and G_3 (with the subgraph G_{31} replaced by its equivalent edge) having eight edges.

(iv) The amplitude of a distribution of objects of type X in space of type Y will be denoted as $A_{X,Y}$.

(v) We define d_{nY} through the relation

$$\langle n(L)\rangle \sim L^{d_{nY}}, \tag{1}$$

where $\langle n(L)\rangle$ is the average number of disjoint objects of a given type in space Y.

(vi) The denote spaces of type X or Y, we use 0,1,2,3 . . . to denote k-blocks with $k=0,1,2,3\ldots$ corresponding to Euclidean space, clusters, blobs, and 3-blocks, respectively. We use B to denote the percolation cluster backbone.

(vii) Additionally, because, as noted above, objects such as 3-blocks can be nested, we denote quantities that relate to all levels of nesting with an asterisk. Specifically, $\tau^*_{X,Y}$ and $A^*_{X,Y}$ denote the exponent of the power-law regime and the amplitude of a distribution of nested objects of type X at all levels of nesting in space of type Y. Similarly, d^*_{nY} is defined through the relation

$$\langle n^*(L)\rangle \sim L^{d^*_{nY}}, \tag{2}$$

where $\langle n^*(L)\rangle$ is the average number of nested objects at all levels of nesting of a given type in space Y. Quantities not qualified with an asterisk will denote quantities at a single level or quantities that cannot be nested.

Using this notation, previous results are [5]

$$n(N_2,L_B)=A_{2,B}L^{d_{nB}}N_2^{-\tau_{2,B}}f_{L2}\left(\frac{N_2}{L^{d_2}}\right) \tag{3}$$

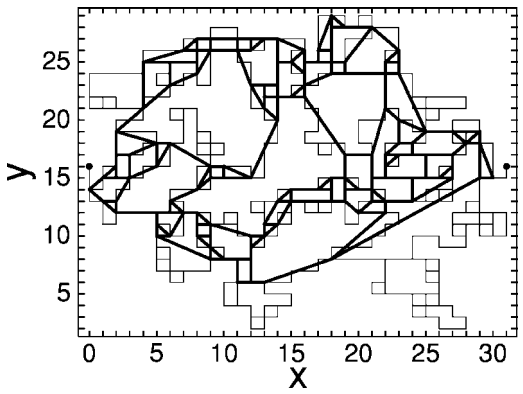

FIG. 2. Example of decomposition of backbone into 3-blocks. The thin lines represent the bonds in the backbone between points {0,15} and {31,15} on a lattice with $L=32$. The backbone is composed of a few single bond blobs connected to the terminal points and a single large blob containing 950 bonds. The thick lines represent the virtual bonds of a single top-level 3-block into which the blob has been decomposed. This 3-block contains 216 virtual bonds. Some of the groups of bonds replaced by virtual bonds can themselves be decomposed into lower-level 3-blocks and so on.

for the number distribution of blobs of mass N_2 in the percolation cluster backbone and [4]

$$n(N_2,L_1)=A_{2,1}L^{d_{n1}}N_2^{-\tau_{2,1}}f_{L2}\left(\frac{N_2}{L^{d_2}}\right) \tag{4}$$

for the number distribution of blobs of mass N_2 in the whole percolation cluster. The finite-size scaling function $f_{L2}(x)$ in Eqs. (3) and (4) approaches 0 when $x>1$ and is 1 otherwise.

In analogy with Eqs. (3) and (4) we expect the number distribution of 3-blocks at all levels of nesting in a blob to be

$$n^*(N_3,L_2)=A^*_{3,2}L^{d^*_{n2}}N_3^{-\tau^*_{3,2}}f_c\left(\frac{N_3}{c}\right)f_{L3}\left(\frac{N_3}{L^{d_3}}\right), \tag{5}$$

where c is the mass of the smallest 3-block and the finite-size scaling function $f_c(x)$ approaches 0 when $x<1$ and is 1 otherwise, reflecting the fact that there cannot be any 3-blocks smaller than the smallest size c. In all dimensions and for all lattices, $c=5$. For simplicity we will approximate $n^*(N_3,L_B)$ as

$$n^*(N_3,L_2)=\begin{cases} A^*_{3,2}L^{d^*_{n2}}N_3^{-\tau^*_{3,2}}, & c\leqslant N_3\leqslant aL^{d_2} \\ 0 & \text{otherwise.}\end{cases} \tag{6}$$

III. SIMULATIONS

We perform simulations with $p=0.5$, the exact percolation threshold for 2D [2,3] and $p=0.248\,812\,6$, the most precise current estimate for the percolation threshold for 3D [8]. We created percolation clusters, which included the sites $(0,L/2)$ and $(L,L/2)$ for the 2D simulations and the sites $(0,L/2,L/2)$ and $(L,L/2,L/2)$ for the 3D simulations, decomposed the backbones determined by these sites into blobs and then decomposed the blobs into 3-blocks. We study both dis-

tributions of 3-blocks in blobs of given mass N_2, and distributions of 3-blocks in backbones in systems of a given size L. For purposes of analysis, we group together blobs with mass $2^{m-1}<N_2\leqslant 2^m$.

We perform the decomposition into 3-blocks along the lines of the procedure sketched in Ref. [6]. Basically, this procedure is as follows: We first designate the blob that we are decomposing as the 2-block graph G. The natural next level of decomposition is to identify connected subgraphs with two or more edges that are connected to G at only two vertices. We denote these subgraphs $G_1, G_2, G_3, \ldots$ of G as two-terminal objects. These two-terminal objects can then be replaced in G by "virtual edges," $e_1, e_2, e_3, \ldots$. Note that this process can be continued recursively. That is, the subgraph G_i may itself contain sub-graphs, $G_{i1}, G_{i2}, G_{i3}, \ldots$ that are connected to G_i at only two vertices; we then replace the subgraphs G_{ij} in G_i by virtual edges e_{Gij}. The process continues until the only remaining subgraphs are those that cannot be decomposed further by making cuts at two vertices; these, by definition, are 3-blocks. An example of this decomposition is shown in Fig. 1. Other methods of decompostion into 3-blocks are described in Refs. [9,10].

We perform at least 3700 realizations for each system size; for the smaller system sizes for which the simulations run more quickly we performed as many as 10^8 realizations. Because, the larger the systems the larger the number of 3-blocks contained in the system, the statistics for the larger systems were acceptable despite the lower number of realizations. We bin the results for all system sizes in order to smooth the plots.

IV. TWO SPATIAL DIMENSIONS

In this section we discuss our results for 3-blocks in 2D percolation. Results in 3D are analogous and are discussed in the following section.

A. 3-blocks in blobs

Figure 3(a) plots the distributions $P^*(N_3|N_2)$, the probability that a 3-block contained in a blob of size N_2 contains N_3 bonds, for various values of N_2. $P(N_3|N_2)$ is the number distribution $n^*(N_3,N_2)$ normalized to unity. Consistent with Eqs. (5) and (6), the plots exhibit power-law regimes followed by cutoffs due to the finite size of the blobs. The "bumps" in the distributions right before the cutoffs represent 3-blocks that would have been larger but are truncated due to the finite size of the blobs in which they are embedded. We estimate the slope of the power-law regimes, $\tau^*_{3,2}$, to be 2.35 ± 0.05. Since

$$N_3 \sim L^{d_3} \tag{7}$$

and

$$N_2 \sim L^{d_2}, \tag{8}$$

we expect

$$N_3 \sim {N_2}^{d_3/d_2}. \tag{9}$$

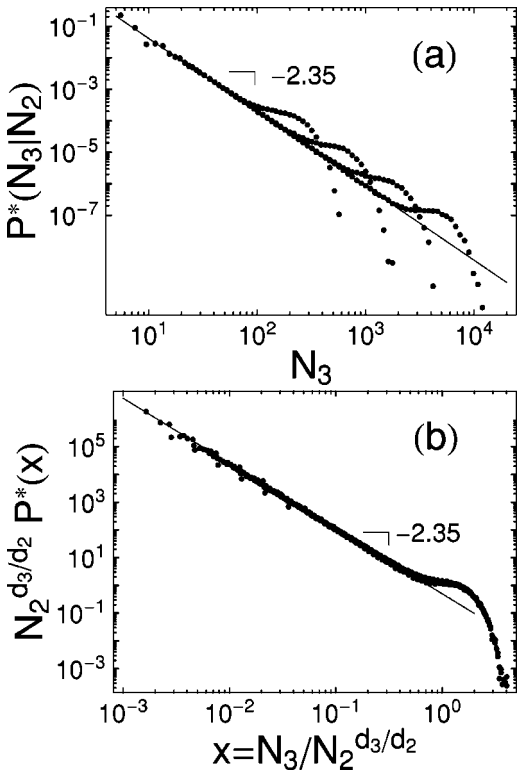

FIG. 3. 2D (a) distributions $P^*(N_3|N_2)$ of the number of 3-blocks of mass N_3 in a blob of size N_2 versus N_3 for (from bottom to top) $N_2=2^{10},2^{12},2^{14}$, and 2^{16}. The distributions exhibit a power-law regime with slope -2.35 ± 0.05 (b) Distributions for $N_2=2^{12},2^{13},2^{14},2^{15}$, and 2^{16} scaled with the value 1.20 for the fractal dimension d_3 which gives the best collapse of the plots in (a).

In Fig. 3(b), we show the collapsed plots in which we scale the distributions by ${N_2}^{d_3/d_2}$ using the most precise published estimate for d_2, 1.6432 ± 0.0008 [11]. (A consistent more recent estimate, $d_2=1.6431\pm 0.0006$, is given in Ref. [12].) Visually, we find the best collapse is obtained for $d_3=1.20\pm 0.1$.

We can also estimate d_3 using Eq. (A5) from the Appendix

$$d_3(\tau^*_{3,2}-1)=d^*_{n2}=d_2. \tag{10}$$

Using $\tau^*_{3,2}=2.35\pm 0.05$ and $d_2=1.6432\pm 0.0008$, results in an estimate of $d_3=1.22\pm 0.05$.

B. 3-blocks in backbone

Figure 4(a) plots the distributions $P^*(N_3|L_B)$, the probability that a 3-block contained in the backbone of a system of size L contains N_3 bonds, for various values of L. $P^*(N_3|L_B)$ is the number distribution $n^*(N_3,L_B)$ normalized to unity. Consistent with Eqs. (5) and (6), the plots exhibit power-law regimes followed by cutoffs due to the finite size of the systems. We estimate the slope of the power- law regimes, $\tau^*_{3,B}$, to be 2.25 ± 0.05. In Fig. 4(b), we

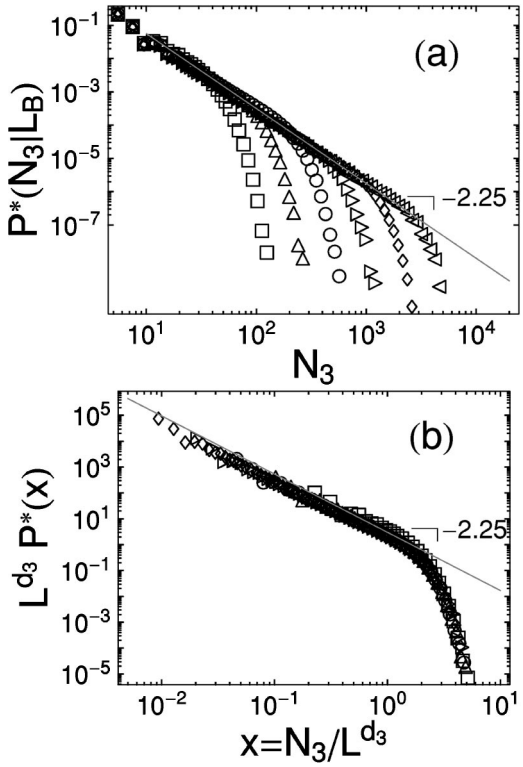

FIG. 4. 2D (a) distributions $P^*(N_3|L)$ of the number of 3-blocks of mass N_3 in a backbone of size L versus N_3 for (from bottom to top) $L=16$, 32, 64, 128, 256, and 512. The distributions exhibit a power-law regime with slope -2.25 ± 0.05 (b) Distributions scaled with the value 1.15 for the fractal dimension d_3 that gives the best collapse of the plots in (a).

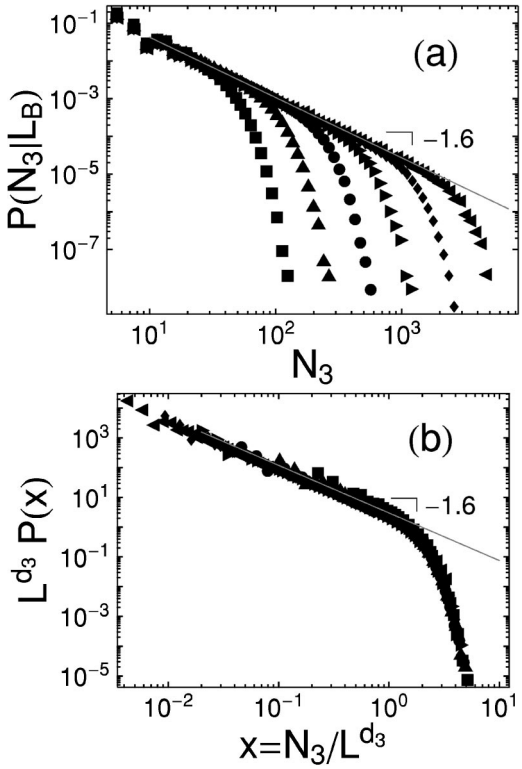

FIG. 5. 2D (a) distributions $P(N_3|L)$ of the number of top level 3-blocks of mass N_3 in a backbone of size L versus N_3 for (from top to bottom) $L=8$, 16, 32, 64, and 128. The distributions exhibit a power-law regime with slope -1.6 ± 0.1. (b) Distributions scaled with the value 1.15 for the fractal dimension d_3 that gives the best collapse of the plots in (a).

show the collapsed plots in which we scale the distributions by L^{d_3}. Visually, we find the best collapse is obtained for $d_3=1.15\pm0.1$.

Next we consider the distribution of ''top-level'' 3-blocks in the backbone. Top-level 3-blocks are those not contained within another 3-block. In Fig. 5(a), we plot the distributions $P(N_3|L_B)$, the probability that a top-level 3-block contained in the backbone of a system of size L contains N_3 bonds, for various values of L. The plots exhibit power-law regimes followed by cutoffs due to the finite size of the systems. The exponent of the power-law regimes $\tau_{3,B}$ is estimated to be 1.6 ± 0.05. In Fig. 5(b), we show the collapsed plots, in which we scale the distributions by L^{d_3}. The best collapse is obtained for $d_3=1.15\pm0.1$, the same value as for the distributions of 3-blocks of all levels. Thus the fractal dimensions of the top-level 3-blocks is the same as the fractal dimension of 3-blocks of all levels but the slopes of the power-law regimes are different; this is seen also in Fig. 6.

We can also use Eq. (A10)

$$d_3(\tau_{3,B}-1)=d_{nB}=\frac{1}{\nu} \tag{11}$$

to obtain an estimate of d_3. Since d_{nB} is known exactly in two dimensions and has been well studied in higher dimensions and because one can usually determine the slope $\tau_{3,B}$ more accurately than d_3 can be determined by finding the best scaling collapse, we determine d_3 more accurately by solving Eq. (11) for d_3. Using our estimate for $\tau_{3,B}$ above we find $d_3=1.25\pm0.1$. Combining this result with our earlier estimates, we make the final estimate

$$d_3=1.20\pm0.1. \tag{12}$$

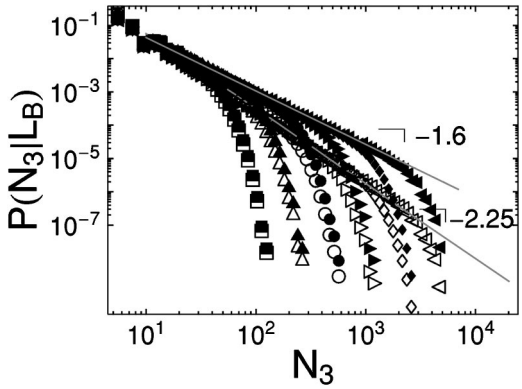

FIG. 6. 2D distributions $P(N_3|L)$ of top-level 3-blocks (filled symbols) and $P^*(N_3|L)$ of all-level 3-blocks (unfilled symbols). While the slopes of the power-law regimes of the two types of distributions are different, the finite-size-system cutoffs are essentially superimposed, consistent with the fractal dimension of the two types of distributions being equal.

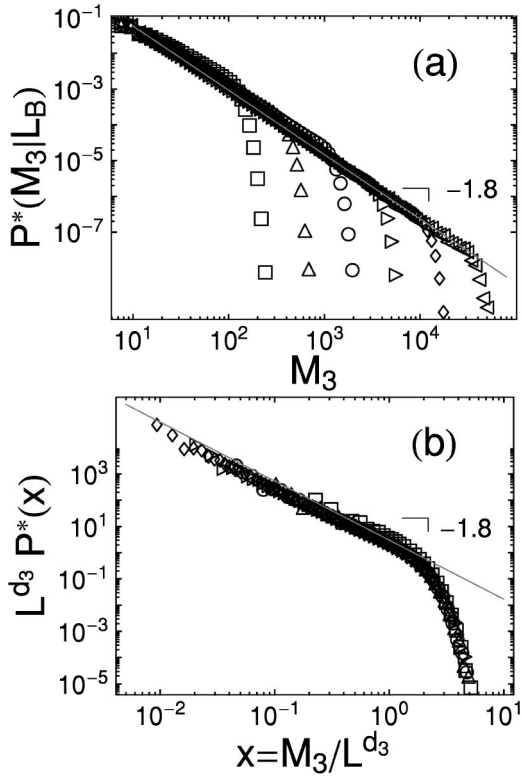

FIG. 7. 2D (a) distributions $P^*(M_3|L)$ of the number of 3-blocks of mass M_3 in a backbone of size L versus M_3 for from top to bottom) $L=16$, 32, 64, 128, 256, and 512. In M_3 we count not virtual bonds but all bonds in the 3-block. The distributions exhibit a power-law regime with slope -1.8 ± 0.1 (b) Distributions scaled with the value 1.6 for the fractal dimension d_3 that gives the best collapse of the plots in (a).

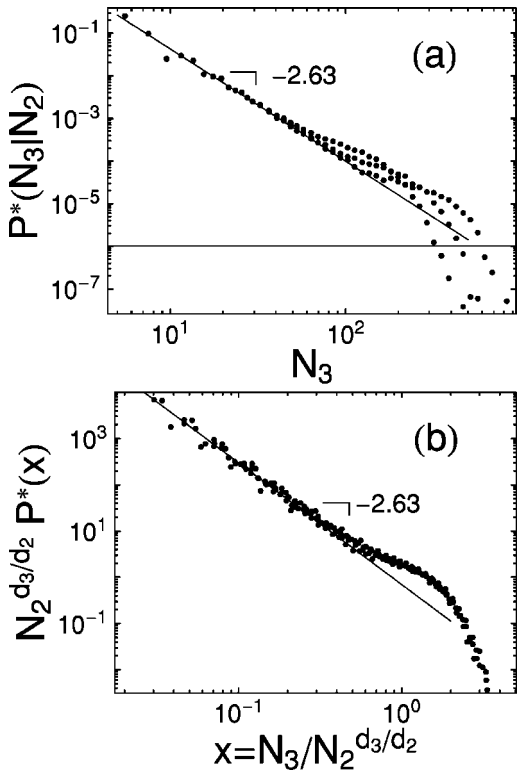

FIG. 8. 3D (a) distributions $P^*(N_3|N_2)$ of the number of 3-blocks of mass N_3 in a blob of size N_2 versus N_3 for (from bottom to top) $N_2=2^{11},2^{12}$, and 2^{13}. The distributions exhibit a power-law regime with slope -2.63 ± 0.05 (b) Distributions for $N_2=2^{11},2^{12}$, and 2^{13} scaled with the value 1.15 for the fractal dimension d_3 that gives the best collapse of the plots in (a).

C. Why the fractal dimension of 3-blocks is smaller than the fractal dimension of the backbone and 2-blocks

The fractal dimension of the 3-blocks is considerably smaller than the fractal dimension, $d_B=1.6432\pm0.0008$ [11], of 2-blocks (blobs). This is because virtual bonds (which are counted as one bond) replace many bonds in the object which it replaces. This can be seen if we plot the distributions $P^*(M_3|L_B)$, the probability that a 3-block contained in the backbone of a system of size L contains M_3 bonds where we can count not the virtual bonds, but all bonds contained a 3-block. In Fig. 7(a) we plot $P^*(M_3|L_B)$ for various L. The best collapse for these plots [Fig. 7(b)] corresponds to a fractal dimension of 1.6 ± 0.1 consistent with the fractal dimension of 2-blocks in 2D. This can be understood as a reflection of the fact that in a system of size L, the mass of the largest 3-block (counting all bonds) can be the same as the backbone mass. This is similar to the situation with blobs and backbones; the largest blob in a backbone can be as large as the whole backbone, which explains why the fractal dimension of blobs is the same as the fractal dimension of the backbone.

Replacing a group of bonds by a virtual bond is analogous to removing dangling ends on a cluster when determining the backbone.

V. THREE SPATIAL DIMENSIONS

Our analysis of the results of the 3D simulations proceeds in a similar manner to the analysis for 2D.

A. 3-blocks in blobs

Figure 8(a) plots the distributions $P^*(N_3|N_2)$, the probability that a 3-block contained in a blob of size N_2 contains N_3 bonds, for various values of N_2. We estimate the slope of the power-law regimes, $\tau^*_{3,2}$, to be 2.63 ± 0.05. In Fig. 8(b), we show the collapsed plots in which we scale the distributions by $N_2^{d_3/d_2}$ with $d_2=1.87\pm0.03$ [13]. Visually, we find the best collapse is obtained for $d_3=1.15\pm0.1$.

Estimating d_3 using Eq. (A5) from the Appendix,

$$d_3(\tau^*_{3,2}-1)=d^*_{n2}=d_2, \tag{13}$$

with $\tau^*_{3,2}=2.63\pm0.05$ and $d_2=1.87\pm0.03$, results in an estimate of $d_3=1.15\pm0.05$.

B. 3-blocks in backbone

Figure 9(a) plots the distributions $P^*(N_3|L_B)$, the probability that a 3-block contained in the backbone of a system of size L contains N_3 bonds, for various values of L. We estimate the slope of the power-law regimes, $\tau^*_{3,B}$, to be 2.55 ± 0.05. In Fig. 9(b), we show the collapsed plots in

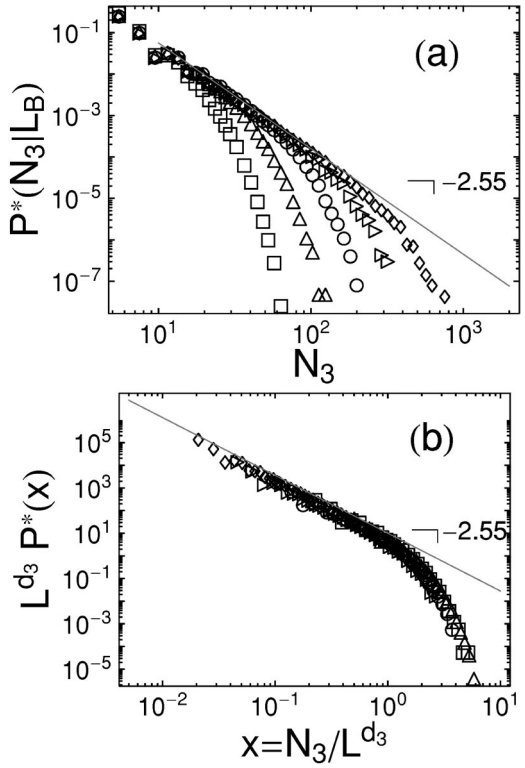

FIG. 9. 3D (a) distributions $P^*(N_3|L)$ of the number of 3-blocks of mass N_3 in a backbone of size L versus N_3 for (from top to bottom) $L=8$, 16, 32, 64, and 128. The distributions exhibit a power-law regime with slope -2.55 ± 0.1. (b) Distributions scaled with the value 1.15 for the fractal dimension d_3 that gives the best collapse of the plots in (a).

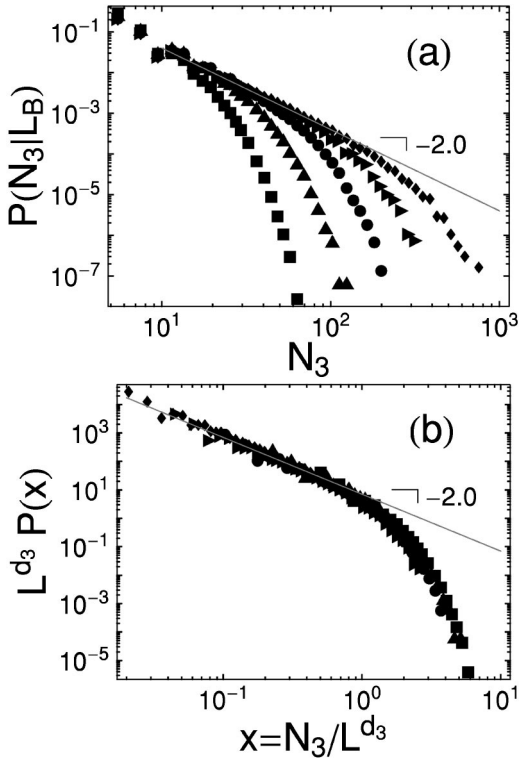

FIG. 10. 3D (a) distributions $P(N_3|L)$ of the number of top-level 3-blocks of mass N_3 in a backbone of size L versus N_3 for (from top to bottom) $L=32$, 64, 128, 256, and 512. The distributions exhibit a power-law regime with slope -2.0 ± 0.1. (b) Distributions scaled with the value 1.15 for the fractal dimension d_3 that gives the best collapse of the plots in (a).

which we scale the distributions by L^{d_3}. Visually, we find the best collapse is obtained for $d_3=1.15\pm0.1$.

Next we consider the distribution of the ''top-level'' 3-blocks in the backbone. In Fig. 10(a), we plot the distributions $P(N_3|L_B)$, the probability that a top-level 3-block contained in the backbone of a system of size L contains N_3 bonds, for various values of L. The exponent of the power-law regimes $\tau_{3,B}$ is estimated to be 2.0 ± 0.05. In Fig. 10(b), we show the collapsed plots, in which we scale the distributions by L^{d_3}. The best collapse is obtained for $d_3=1.15\pm0.1$, the same value as for the distributions of 3-blocks of all levels. As in 2D, the fractal dimensions of the top level 3-blocks is the same as the fractal dimension of 3-blocks of all levels but the slopes of the power-law regimes are different; this is seen also in Fig. 11.

Using Eq. (A10)

$$d_3(\tau_{3,\mathrm{B}}-1)=d_{nB}=\frac{1}{\nu}. \tag{14}$$

To obtain an estimate of d_3 with our estimate for $\tau_{3,B}$ above we find $d_3=1.14\pm0.1$. Combining this result with our earlier estimates, we make the final estimate

$$d_3=1.15\pm0.1. \tag{15}$$

The simulation results notwithstanding, it would be surprising if d_3 were smaller in 3D than in 2D because, below the critical dimension $d_c=6$, both the fractal dimensions of clusters and blobs increase with the Euclidean dimension. This suggests that while the actual values of d_3 may be within the bounds we have estimated, the actual values will be consistent with d_3 (2D)$\leqslant d_3$ (3D).

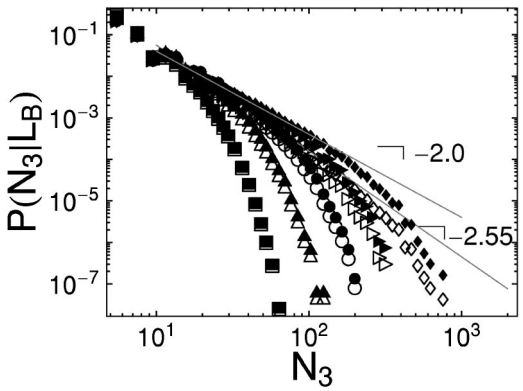

FIG. 11. 3D distributions $P(N_3|L)$ of top-level 3-blocks (filled symbols) and $P^*(N_3|L)$ of all-level 3-blocks (unfilled symbols). While the slopes of the power-law regimes of the two types of distributions are different, the finite-size-system cutoffs are essentially superimposed consistent, with the fractal dimension of the two types of distributions being equal.

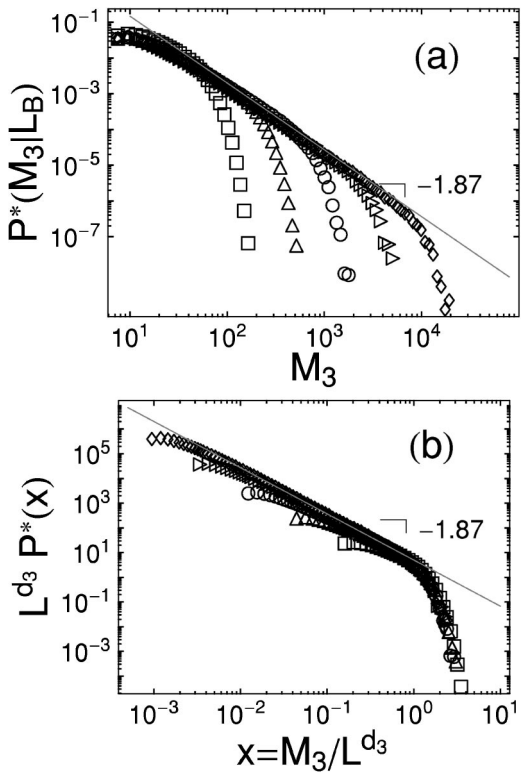

FIG. 12. 3D (a) distributions $P^*(M_3|L)$ of the number of 3-blocks of mass M_3 in a backbone of size L versus M_3 for (from top to bottom) $L=8$, 16, 32, 64, and 128. In M_3 we count not virtual bonds but all bonds in the 3-block. The distributions exhibit a power-law regime with slope -1.87 ± 0.1. (b) Distributions scaled with the value 1.85 for the fractal dimension d_3 that gives the best collapse of the plots in (a).

As in 2D, if we do not replace two-terminal objects in a 3-block by a single virtual bond, the fractal dimension of the 3-block is that of a blob (see Fig. 12).

Estimates for all of the 2D and 3D exponents are summarized in Table I.

VI. DECOMPOSITION OF THE WHOLE PERCOLATION CLUSTER

While we have only decomposed 2-blocks that comprise the cluster backbone, we could proceed similarly for all 2-blocks into which a cluster is decomposed. The fractal dimension of the 3-blocks into which a cluster is ultimately decomposed should be the same as the fractal dimension of the 3-blocks into which the backbone is ultimately decomposed. The only difference we would expect in our results would be that the slope of the power-law regime of the distribution of the top-level 3-blocks would be given by

$$d_3(\tau_{3,1}-1)=d_{n1}=d, \tag{16}$$

the analogy of Eq. (A10)

VII. *k*-BONES AND PATH CROSSING PROBABILITIES

Just as blobs and backbones have the same fractal dimension, we can identify objects analagous to backbones which have the same fractal dimensions as *k*-blocks. We define a *k*-bone as the set of all points in a percolation system connected to *k* disjoint terminal points (or sets of disjoint terminal points) by *k* disjoint paths. Thus the backbone is a *k*-bone with $k=2$. Just as the largest *k*-blocks into which a backbone can be decomposed are 2-blocks, the largest *k*-blocks into which a *k*-bone can be decomposed are *k*-blocks. The fractal dimension of *k*-bones is the fractal dimension of the *k*-blocks. One can see this easily by noting that if the *k*-terminal points that define a *k*-bone are connected to each other, the resulting structure is *k*-block.

TABLE I. Measured fractal dimension, measured power-law regime exponent, and calculated fractal dimension for 3-blocks in 2D and 3D. The calculated value of d_3 is determined by Eq. (10) for 3-blocks in a blob and Eq. (11) for 3-blocks in the backbone.

	d_3 Measured	τ Measured	d_3 Calculated
	2D		
All 3-blocks in blob	1.20 ± 0.1	2.35 ± 0.05	1.22 ± 0.05
All 3-blocks in backbone	1.15 ± 0.1	2.25 ± 0.05	—
Top-level 3-blocks in backbone	1.15 ± 0.1	1.60 ± 0.05	1.25 ± 0.1
	3D		
All 3-blocks in blob	1.15 ± 0.1	2.63 ± 0.05	1.15 ± 0.05
All 3-blocks in backbone	1.15 ± 0.1	2.55 ± 0.05	—
Top-level 3-blocks in backbone	1.15 ± 0.1	2.0 ± 0.05	1.14 ± 0.1

Recent work [14] has identified a relationship between path crossing probabilities and the fractal dimensions of percolation structures. Specifically, consider the probability, $\hat{P}_k^P$ that in an annular region the small inner circle of radius r is connected to the larger outer circle of radius R, $R\gg r$, by k disjoint paths. Then

$$\hat{P}_k^P \sim \left(\frac{r}{R}\right)^{\hat{x}_k}. \tag{17}$$

It has been observed [14] that $\hat{x}_1$ is the codimension of the percolation cluster and $\hat{x}_2$ is the codimension of the backbone. We extend these observations to the case of general *k*

$$d-\hat{x}_k=d_k, \tag{18}$$

where d is the spatial dimension of the system. This should hold in all dimensions where the annulus is now defined by two hyperspheres. It has been argued [12] that

$$x_k<\hat{x}_k<x_{2k}, \tag{19}$$

where x_k is the polychromatic path crossing exponent [14] and which has been found rigorously in 2D to be [14]

$$x_k=\tfrac{1}{12}(k^2-1). \tag{20}$$

Using Eqs. (18)–(20), we find in 2D

$$-\tfrac{11}{12}<d_3<\tfrac{4}{3}, \tag{21}$$

consistent with our estimate for d_3 in 2D.

The relationship between the path crossing problem for $k=2$ and the backbone dimension has been recently exploited to determine d_B very accurately using a transfer matrix technique [12]. Possibly similar methods can be employed to find the fractal dimension of k-bones (and therefore k-blocks) with $k \geqslant 3$ to high precision.

VIII. RELATIONSHIP TO RENORMALIZATION GROUP

The process of replacing a two-terminal object t by a single virtual bond and then replacing two-terminal objects within t by single virtual bonds and so on is reminiscent of the decimation process in renormalization group (RG) approaches to percolation [2,3,15,16]. It is here, however, that the similarity ends. The decimation process performed in the decomposition into 3-blocks is an exact decimation performed on objects in individual realizations while the RG decimation is performed on the lattice and is an approximation, except for hierarchical lattices. Also, the purpose of the decomposition into 3-blocks is to improve computational performance and analyze the properties of substructures of the cluster while the purpose of RG calculations is to find properties of percolation analytically. Finally, whereas RG approaches on hierarchical lattices result in objects that are finitely ramified, the decomposition into 3-blocks we perform maintains the infinite ramification of the Euclidean lattice.

IX. COMPUTATIONAL IMPLICATIONS

The fact that the fractal dimension of 3-blocks is significantly smaller than the fractal dimension of 2-blocks has important computational implications. We can efficiently calculate properties (e.g., resistance, velocity distributions, self-avoiding walk statistics) of a percolation cluster or backbone as follows: (i) decompose the cluster or backbone into 2-blocks; (ii) decompose the 2-blocks into 3-blocks; (iii) calculate the desired properties of the 3-blocks; (iv) algebraically determine the properties of the 2-blocks from the properties of the 3-blocks; and (v) algebraically determine the properties of the cluster or backbone from the properties of the 2-blocks.

In many cases the computation will require less CPU (computer processing) resource when the complexity of the computation is a power law or exponential of the mass of the object for which the property is being calculated. By decomposition we make the mass of these objects smaller. Reduced CPU resource usage is also obtained if only a decomposition into 2-blocks is made although the saving is less. Systems of larger size than that could be treated before can now be treated when we decompose into 3-blocks because the fractal dimension of the 3-blocks is lower than that of the backbone in which they are embedded; this is not true if we only decompose into 2-blocks.

As an example of the dramatically smaller size of the largest 3-block versus the size of the largest blob consider a 3D system of size $L=1000$. At criticality, the largest mass blob in the backbone will be of the order $L^{1.62} \approx 63\,000$ while the mass of the largest 3-block in the backbone will be of $L^{1.2} \approx 4000$. In Fig. 2 we show an actual simulation realization in which a blob of 950 bonds is decomposed into a 3-block with only 216 virtual bonds, greatly reducing the computational complexity.

X. DISCUSSION

Traditionally the decomposition of percolation systems has been to decompose the system into clusters (1-blocks) and to decompose the clusters into blobs (2-blocks). We extend this decomposition by decomposing 2-blocks into 3-blocks. 3-blocks are especially interesting because in contrast to 1- and 2-blocks, the 3-blocks have the property that they can be nested. That is, two-terminal objects, which are replaced by single virtual bonds in a 3-block, can themselves contain other 3-blocks. Because of this replacement of a 2-terminal object by a virtual bond, the fractal dimension of 3-blocks is significantly smaller than the fractal dimension of 2-blocks. As discussed in the preceding section, this smaller fractal dimension has important computational implications for the size of percolation systems, which can be analyzed and the speed at which the analysis can be performed.

In addition, within the error bars of our calculations, the values for the 3-block fractal dimension appear to be identical for 2D and 3D systems. Simulations of larger systems and higher-dimension systems could help answer whether in fact d_3 is independent of dimension (superuniversal). It will also be of interest to determine the properties of k-blocks with $k>3$.

ACKNOWLEDGMENTS

We thank D. Baker, L. Braunstein, S. Havlin, A. Moreira, V. Schulte-Frohlinde, and D. Stauffer for stimulating discussions and helpful comments.

APPENDIX A: RELATIONSHIPS AMONG EXPONENTS

Here we ask if any of the fractal dimensions and power-law regime exponents we have identified are related. To answer this question we must first briefly review some existing results for relations between other exponents.

1. Previous results

It has been shown generally [17,18] that, for disjoint objects of type X embedded in a space Y,

$$d_X(\tau_{X,Y}-1)=d_{nY}. \tag{A1}$$

Equation (A1) holds if $\tau_X<2$ or if d_{nY} is equal to the fractal dimension of space Y, d_Y.

Special cases of Eq. (A1) have been identified previously for $Y=0$, 1, and 2 corresponding to Euclidean space, percolation cluster space, and percolation backbone space, respectively.

(i) The first is the familiar scaling relation for the Fisher exponent τ [2,3]

$$d_f(\tau-1)=d_{n0}=d \qquad \text{(clusters)}, \tag{A2}$$

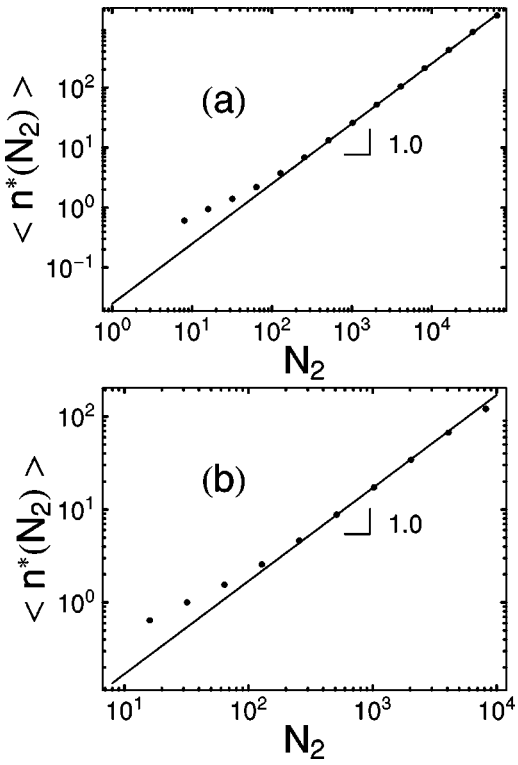

FIG. 13. $\langle n^*(N_2)\rangle$, the average number of 3-blocks in a blob of size N_2 versus N_2 for (a) 2D and (b) 3D.

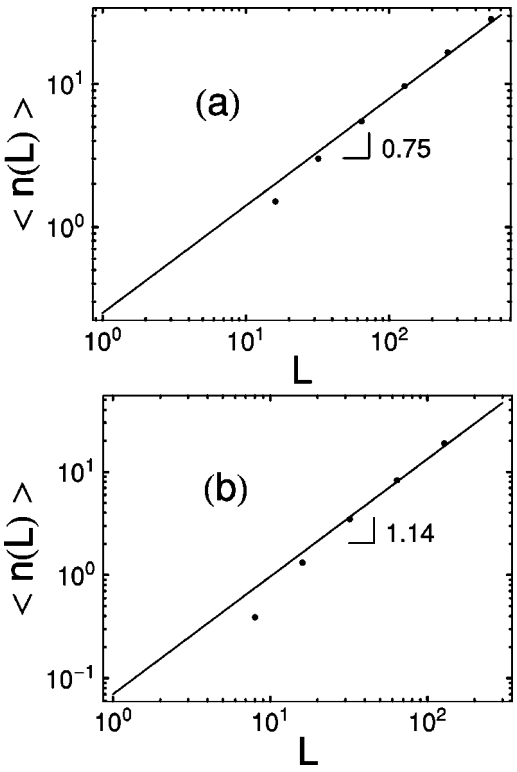

FIG. 14. $\langle n(L)\rangle$, the average number of top-level 3-blocks in a backbone of size L versus L. (a) 2D The solid line has slope 0.75. (b) 3D The solid line has slope 1.14.

where d is the Euclidean dimension, d_f the fractal dimension of the cluster, and τ the exponent of the power-law regime in the distribution of cluster sizes.

(ii) In Ref. [4] it was shown that

$$d_{\text{blob-cl}}(\tau_{\text{blob-cl}}-1)=d_{n1}=d_f, \quad \text{(cluster blobs)}, \quad \text{(A3)}$$

where $d_{\text{blob-cl}}$ and $\tau_{\text{blob-cl}}$ are the fractal dimension and the exponent of the power-law regime, respectively, for all blobs in the cluster.

(iii) In Ref. [5] it was argued that

$$d_{\text{blob-bb}}(\tau_{\text{blob-bb}}-1)=d_{nB}=d_{\text{red}}, \quad \text{(backbone blobs)} \quad \text{(A4)}$$

where $d_{\text{blob-bb}}$ and $\tau_{\text{blob-bb}}$ are the fractal dimension and the exponent of the power-law regime, respectively, for those blobs in the backbone and d_{red} is the fractal dimension of singly connected red bonds in the backbone.

Both $d_{\text{blob-cl}}$ and $d_{\text{blob-bb}}$ are equal to d_B, the backbone fractal dimension. In (i) and (ii), Eq. (A1) applies because $d_{nY}=d_Y$; in (iii), Eq. (A1) applies because $\tau_X<2$.

2. 3-blocks in blobs

In analogy with Eqs. (A2) and (A3), we would expect

$$d_3(\tau^*_{3,2}-1)=d^*_{n2}=d_2. \quad \text{(A5)}$$

We first confirm that the total number of 3-blocks in blobs scales with the exponent d_2. If

$$\langle n(L)\rangle \sim L^{d_{n2}} \quad \text{(A6)}$$

and

$$N_2 \sim L^{d_2}. \quad \text{(A7)}$$

Then we would expect

$$\langle n(N_2)\rangle \sim L^{d_{n2}/d_2}. \quad \text{(A8)}$$

Figures 13(a) and 13(b) are log-log plots of $\langle n(N_2)\rangle$, the average number of all 3-blocks in a blob, versus blob size N_2 for 2D and 3D, respectively. The straight line fits with slope 1.0 ± 0.05 are consistent with $d_{n2}=d_2$. Our simulation results in 2D from Sec. IV, $d_3=1.20$ and $\tau_{3,2}=2.35$ result in $d_3(\tau^*_{3,2}-1)=1.62$ close to the value $d_2=1.6432$. In 3D, our simulation results from Sec. V, $d_3=1.15$ and $\tau_{3,2}=2.63$ result in $d_3(\tau^*_{3,2}-1)=1.87$ identical to the value $d_2=1.87$ [13].

3. 3-blocks in backbone

Because the number of top-level 3-blocks in the backbone is proportional to the number of 2-blocks in the backbone, the number of top level 3-blocks in the backbone should scale the same way the number of 2-blocks in the backbone. For all dimensions and lattices, d_{nB} has been shown to be [19,20]

$$d_{nB}=d_{red}=\frac{1}{\nu}, \quad \text{(A9)}$$

where ν is the exponent associated with the divergence of the correlation length as p approaches p_c [1,2]. In 2D $1/\nu$ is exactly 3/4 [21,22]; in 3D, $1/\nu$ has been estimated to be 1.143 ± 0.01 [23,24]. We would expect

$$d_3(\tau_{3,\mathrm{B}}-1)=d_{nB}=\frac{1}{\nu}. \tag{A10}$$

Figures 14(a) and 14(b) are log-log plots of $\langle n(L)\rangle$, the average number of top-level 3-blocks in the backbone versus system size L for 2D and 3D, respectively. The straight line fits with slope 0.75 ± 0.05 and 1.14 ± 0.05 are consistent with the exact and previously estimated values for $1/\nu$ of 3/4 and 1.143 in 2D and 3D, respectively. Our 2D simulation results from Sec. IV, $d_3=1.15$ and $\tau_{3,2}=1.60$ result in $d_3(\tau_{3,B}-1)=0.69$ close to the value $1/\nu=3/4$. For 3D, our simulation results from Sec. V, $d_3=1.15$ and $\tau_{3,2}=2.0$ result in $d_3(\tau_{3,B}-1)=1.15$ close to the value $1/\nu=1.143$.

[1] D. Ben-Avraham and S. Havlin, *Diffusion and Reactions in Fractals and Disordered Systems* (Cambridge University Press, Cambridge, 2000).

[2] D. Stauffer and A. Aharony, *Introduction to Percolation Theory* (Taylor & Francis, Philadelphia, 1994).

[3] A. Bunde and S. Havlin, in *Fractal and Disordered Systems*, edited by A. Bunde and S. Havlin (Springer-Verlag, New York, 1996).

[4] M.F. Gyure, M.V. Ferer, B.F. Edwards, and G. Huber, Phys. Rev. E **51**, 2632 (1995).

[5] H.J. Herrmann and H.E. Stanley, Phys. Rev. Lett. **53**, 1121 (1984).

[6] W. T. Tutte, *Graph Theory* (Cambridge University Press, Cambridge, 1984).

[7] The precise definition of a k-block is (previous reference): A graph G is a k-block if it has no n separation for any $n<k$. An n separation of G is a pair of subgraphs of G, H, and K, where (i) $H \cup K = G$, (ii) H and K have exactly k common vertices, and (iii) H and K each have at least k edges.

[8] C.D. Lorenz and R.M. Ziff, Phys. Rev. E **57**, 230 (1998).

[9] W. Hohberg, Discrete Math. **109**, 133 (1992).

[10] J.E. Hopcroft and R.E. Tarjan, SIAM J. Comput. **2**, 135 (1973).

[11] P. Grassberger, J. Phys. A **262**, 252 (1999).

[12] J. Jacobsen and P. Zinn-Justin, e-print cond-mat/0111374. These authors denote $\hat{x}_k$ by $\tilde{x}_k$.

[13] M. Porto, A. Bunde, S. Havlin, and H.E. Roman, Phys. Rev. E **56**, 1667 (1997).

[14] M. Aizenman, B. Duplantier, and A. Aharony, Phys. Rev. Lett. **83**, 1359 (1999). These authors denote $\hat{x}_k$ by $\hat{x}^P_{\not\prime}$.

[15] J.-P. Hovi and A. Aharony, Phys. Rev. E **56**, 172 (1997).

[16] P.J. Reynolds, H.E. Stanley, and W. Klein, Phys. Rev. B **21**, 1223 (1980).

[17] G. Huber, M.H. Jensen, and K. Sneppen, Fractals **3**, 525 (1995).

[18] G. Huber, M.H. Jensen, and K. Sneppen, Phys. Rev. E **52**, R2133 (1995).

[19] H.E. Stanley, J. Phys. A **10**, L211 (1977); A. Coniglio, *ibid.* **15**, 3829 (1982).

[20] A. Coniglio, Phys. Rev. Lett. **46**, 250 (1982).

[21] M.P.M. den Nijs, J. Phys. A **12**, 1857 (1979).

[22] B. Nienhuis, J. Phys. A **15**, 199 (1982).

[23] R. M. Ziff and G. Stell (unpublished).

[24] P.N. Strenski, R.M. Bradley, and J.M. Debierre, Phys. Rev. Lett. **66**, 133 (1991).